

Fuzzy Flight Control System For Decoupling Supersonic Missile

Tain-sou Tsay

Assistant Professor, Department of Aeronautical Engineering, National Formosa University

Abstract

In this literature, a fuzzy control technique is proposed for analyses and designs of a serious aerodynamic coupled skid-to-turn supersonic missile. Fuzzy decoupling logic is developed from conventional design techniques and experiences with two measurable accelerations. It can be easily applied to cope with large single-axis and double-axis maneuvers simultaneously. The fuzzy control system provides simple manner to get same robustness comparing to those of conventional designs technique. All analyzed results are verified by 5-DOF simulations under system variations and uncertainties.

Key Words: Fuzzy control 、 Flight control System 、 Aerodynamic decoupling.

Dr. Tsay is with the Department of Aeronautical Engineering, National Formosa University, No. 64, Wen-Hua Road, HuWei, YunLin, 63208, Taiwan.

Tel:+886-5-631-5537

Fax:+886-5-631-2415

E-mail: ttsay@nfu.edu.tw

I . Introduction

It is well known that aerodynamic couplings from pitching/yawing channels to rolling channels of cruciform skid-to-turn missiles will destabilize or degrade the performance of the system[1,2]. Higher gain crossover frequency ratios of the rolling channel to pitching/ yawing channels for decoupling are usually expected. They are usually used in conventional design techniques [3, 4], and are diagonal dominant designs for multivariable feedback systems[5,6]. They are disturbance rejection designing techniques. However, it is constrained by hardware dynamics, especially for bandwidth-limited fin actuators.

Furthermore, aerodynamic couplings from pitching / yawing channels to rolling channels are classified into unstable and stable aerodynamic couplings. The unstable- coupling decreases the gain crossover frequency of the rolling channel, while the stable coupling increases the gain crossover frequencies. They are corresponding to large single-axis and large double-axis maneuvers, respectively for cruciform missile. However, small maneuvers are almost not disturbing the gain crossover frequencies. Therefore, complicated gain adaptations according to magnitudes of maneuvers to keep almost constant gain crossover frequency are usually required.

They are call gain logic and usually need vast mathematic evaluations. In this work, fuzzy gain logic is used on-line or off-line and gives simple manner to describe small / large unstable / stable couplings and large/small gain adaptations for the rolling loop automatically. Other possible methods are to use cross- decoupling controllers[7-9], output feedback- decoupling controllers[10,11] and Dynamic Inversion (DI) methods[12-18]. In general, inverting the transfer function matrix of plant for missile flight control system suffers from it has large modeled, un- modeled uncertainties, non- minimum-phase zeros and large faster variations of cross-coupling dynamics.

This literature is organized as follows: effects of aerodynamic couplings are discussed and classified in Section II; conventional designs are discussed and applied in Section III; the proposed fuzzy logic is applied to the considered system in Section IV; and 5DOF simulations verification are performed. It will be seen that the fuzzy flight control system provides simple manner to get same robustness comparing to those of conventional designs technique. All analyzed results will be verified by 5-DOF simulations under system variations and uncertainties.

II . The Coupling Effects

The translational and rotational dynamics of the missile shown in Fig.1 are described by the following

six nonlinear differential equations[19]:

$$\dot{U} = -\frac{\bar{q}\bar{s}}{m}C_x - WQ + VR + \frac{F_{xg}}{m} \quad (1)$$

$$\dot{V} = -\frac{\bar{q}\bar{s}}{m}C_y - UR + WP + \frac{F_{yg}}{m} \quad (2)$$

$$\dot{W} = -\frac{\bar{q}\bar{s}}{m}C_z - VP + UQ + \frac{F_{zg}}{m} \quad (3)$$

$$\dot{P} = -\frac{l}{I_x}C_l\bar{q}\bar{s}l \quad (4)$$

$$\dot{Q} = C_m\bar{q}\bar{s}l - \frac{(I_x - I_z)}{I_y}PR \quad (5)$$

$$\dot{R} = C_n\bar{q}\bar{s}l - \frac{(I_y - I_x)}{I_y}PQ \quad (6)$$

In above equations, U , V and W are velocity components measured on the missile body axes; P , Q and R are the components of the body angular rate: F_{xg} , F_{yg} , F_{zg} are the gravitational forces acting along the body axes: and I_x , I_y , I_z are the moments of inertia. The variable \bar{s} is the reference area, \bar{q} is the dynamic pressure

$$\bar{q} = \frac{1}{2}\rho(U^2 + V^2 + W^2) \equiv \frac{1}{2}\rho V_M^2 \quad (7)$$

l is the reference length. The aerodynamic lifting forces (C_x, C_y, C_z) and moments (C_l, C_m, C_n) are function of Mach number, angle of attack (α^*), angle of sideslip (β^*); the angles of attack and sideslip are defined as

$$\alpha^* = \tan^{-1}\left(\frac{W}{U}\right) \quad (8)$$

and

$$\beta^* = \tan^{-1}\left[\sin^{-1}\left(\frac{V}{V_M}\right) / \cos \alpha^*\right] \quad (9)$$

The small signal perturbation model from a specified set of trim conditions ($P^*, Q^*, R^*, A_{z0}, A_{y0}, \alpha^*, \beta^*$) is described by following differential equations:

$$\dot{p} = L_p p + L_\alpha \alpha + L_\beta \beta + L_{\delta p} \delta p + L_{\delta q} \delta q + L_{\delta r} \delta r \quad (10)$$

$$\dot{q} = M_q q + M_\alpha \alpha + M_{\delta q} \delta q + M_{\delta p} \delta p \quad (11)$$

$$\dot{r} = N_r r + N_\beta \beta + N_{\delta r} \delta r + N_{\delta p} \delta p \quad (12)$$

$$\dot{\alpha} = -\tan \beta^* p + q + M_B (Z_\alpha \alpha + Z_{\delta q} \delta q + Z_{\delta p} \delta p) \quad (13)$$

$$\dot{\beta} = \tan \alpha^* p - r + M_B (Y_\beta \beta + Y_{\delta r} \delta r + Y_{\delta p} \delta p) \quad (14)$$

$$a_{zacc} = Z_\alpha \alpha + Z_{\delta q} \delta q + Z_{\delta p} \delta p - l_s (M_q q + M_\alpha \alpha + M_{\delta p} \delta p + M_{\delta q} \delta q) \quad (15)$$

$$a_{yacc} = Y_\beta \beta + Y_{\delta r} \delta r + Y_{\delta p} \delta p + l_S (N_r r + N_\beta \beta + N_{\delta p} \delta p + N_{\delta r} \delta r) \quad (16)$$

where p, q, r are body angular rate deviations from trims (P^*, Q^*, R^*); a_{zacc}, a_{yacc} are body acceleration deviations from trims (A_{ZO}, A_{YO}); and α and β are angles of attack and sideslip deviations from trims (α^*, β^*), l_S is the distance between sensor position and Central of Gravity (CG). $L_{(\bullet)}, M_{(\bullet)}, N_{(\bullet)}, Y_{(\bullet)}$ and $Z_{(\bullet)}$ are derivatives of moments (C_l, C_m, C_n)/ forces (C_y, C_z) with respect to $p, q, r, \alpha, \beta, \delta p, \delta q, \delta r$. Fig. 2 shows connections given by Equations (10) to (16), in which gray blocks show coupling effects between rolling/ yawing/ pitching channels. For large angle of attack (α^*) and small sideslip angle (β^*), the magnitude of terms $\tan \beta^*$ and L_α will much less than those of $\tan \alpha^*$ and L_β , thus the original 3×3 system can be decomposed into a 2×2 roll-yaw coupled system and a pitching system. Similar to the case of large value of β^* and small value of α^* , it can be decomposed into a 2×2 roll-pitch coupled system and a yawing system. In the following paragraph, a 2×2 roll-yaw coupled system and a 2×2 roll-pitch coupled system are used to illustrating aerodynamic coupling effects.

Now, consider the major coupling effects from yawing channel to rolling channel of a 2×2 roll-yaw coupled system. The transfer function of $p/\delta r$ is

$$\frac{p}{\delta r} = \frac{L_{\delta r} s^2 + [L_\beta M_B Y_{\delta r} - L_{dr} (N_r + M_B Y_\beta)] s - L_\beta (N_{\delta r} + Y_{\delta r} M_B N_r)}{s^3 - (L_p + N_r + M_B Y_\beta) s^2 + (L_p N_r + N_\beta + L_p M_B Y_\beta + N_r M_B Y_\beta - \tan \alpha^* L_\beta) s + L_\alpha (N_\beta + N_r M_B Y_\beta) - L_p (N_\beta + N_r M_B Y_\beta) + N_r \tan \alpha^* L_\beta} \quad (17)$$

The denominator of Equation (17) can be approximated by

$$\Delta_{pr}(s) = s^3 - (L_p + N_r + M_B Y_\beta) s^2 + (N_\beta - \alpha^* L_\beta) s - L_p N_\beta + N_r \alpha^* L_\beta \quad (18)$$

for

$$\begin{aligned} \tan \alpha^* &\cong \alpha^* ; \\ |N_\beta - \alpha^* L_\beta| &\gg |L_p N_r + L_p M_B Y_\beta| ; \\ |-L_p N_\beta + N_r \alpha^* L_\beta| &\gg |L_p N_r M_B Y_\beta| \end{aligned}$$

Since the value of N_r is negative for stable static margin(SM), the positive value of $\alpha^* L_\beta$ is called the unstable aerodynamic coupling for it will destabilize or degrade performance of the system; while negative value of $\alpha^* L_\beta$ is called the stable aerodynamic coupling. Note that the magnitude of L_β given in the

numerator of Equation (17) is much greater than that of $L_{\delta r}$. Such that L_β and $\alpha^* L_\beta$ are two major coupling terms. They affect not only the magnitude but also the stability of the system. Equation (17) gives also that the coupling behavior due to L_β and $\alpha^* L_\beta$ will occur in the low-medium frequency band.

Considering another simplified 2×2 roll-pitch coupled system, the transfer function of $p/\delta q$ is in the form of

$$\frac{p}{\delta q} = \frac{L_{\delta q} s^2 + [L_\alpha M_B Z_{\delta q} - L_{dq} (M_q + M_B Z_\alpha)] s + L_\alpha (M_{\delta q} - Z_{\delta q} M_B M_q)}{s^3 - (L_p + M_q + M_B Z_\alpha) s^2 + (L_p M_q - M_\alpha + L_p M_B Z_\alpha + M_q M_B Z_\alpha - \tan \beta^* L_\alpha) s + L_{\delta q} (-M_\alpha + M_q M_B Z_\alpha) - L_p (-M_\alpha + M_q M_B Z_\alpha) - M_q \tan \beta^* L_\alpha} \quad (19)$$

Similar to discussions for the 2×2 roll-yaw coupled system, one can find the approximated denominator of Equation (19) is

$$\Delta_{pq}(s) = s^3 - (L_p + M_q + M_B Z_\alpha) s^2 + (-M_\alpha + \beta^* L_\alpha) s + L_p M_\alpha - M_q \beta^* L_\alpha \quad (20)$$

Equation (20) gives the positive value of $\beta^* L_\alpha$ is called the stable aerodynamic coupling; and negative value of $\beta^* L_\alpha$ is called the unstable aerodynamic coupling. $\beta^* L_\alpha$ and L_α are two major coupling terms from pitching channel to rolling channel. Equation (17) and Equation (19) give that the characteristic of the considered system is largely affected by $\beta^* L_\alpha$ and $\alpha^* L_\beta$. Therefore, the major couplings to rolling channel can be described by

$$T_C = N_r \alpha^* L_\beta - M_q \beta^* L_\alpha \quad (21)$$

Negative value of T_C represents the coupling is unstable and positive value of T_C represents the coupling is stable. Zero value of T_C represents zero coupling. Large value of α^* or β^* is corresponding to large value of A_{ZO} or A_{YO} . They approach to measured accelerations (A_{ZF}, A_{YF}) also. Fig. 3 shows the coupling T_C of the considered system.

It gives stable, unstable and zero aerodynamic couplings. The small perturbed aerodynamic coefficients of the considered system are given in Appendix A [20] for ten typical combinations of angle of attacks (α^*) and sideslip (β^*). Fig.4 shows typical open-loop frequency responses of rolling channel for stable/ unstable/ zero aerodynamic couplings. The flight condition, gains and compensators will be discussed and given in next section. Fig.4 shows gain crossover frequencies are largely affected by aerodynamic couplings. The unstable-coupling destabilizes the system and stable-coupling increasing the gain crossover frequency.

Fig.5 shows the constant- T_C loci with respect to $|A_{ZO}|$ and $|A_{YO}|$. It is redrawn from Fig.3. The shaded-area is the stable aerodynamic coupling region and can be further partitioned into “ZC”, “ZC→SSC”, “SSC”, “SSC→LSC”, “LSC” areas roughly; i.e., from zero-coupling(ZC) through small-stable coupling(SSC) to large- stable coupling (LSC). The other region is the unstable aerodynamic coupling region and can be further partitioned into “ZC→SUC”, “SUC→LUC” and “LUC” areas roughly also; i.e., from zero-coupling(ZC) through small-unstable coupling (SUC) to large-unstable coupling(LUC). The boundaries between areas are ambiguous. It will be seen proper gains of the autopilot are dependent on zero-small-large values of aerodynamic couplings. The gain logic in conventional autopilot according to $|A_{ZO}|$ and $|A_{YO}|$ is very complicated.

III. Conventional Design Techniques

Fig.6 excluding the fuzzy logic block is the conventional well-proven control configuration of missile autopilots[3,4]; in which (K_{opo}, K_{ipo}) , (K_{oq}, W_{iq}, K_{iq}) and (K_{or}, W_{ir}, K_{ir}) are gains of rolling/pitching/yawing channels to be adapted. In general, they are first gain scheduled with missile velocity and altitude. K_{opo} and K_{ipo} are further adapted by values of angles of attack/sideslip; i.e., $K_{ip} = Sckip \times K_{ipo}$ and $K_{op} = Sckop \times K_{opo}$. K_{opo} and K_{ipo} are gains of zero aerodynamic coupling situations. Angles of attack/sideslip are usually replaced by measurable accelerations A_{Zf} and A_{Yr} . In this work, more attentions are paid for large angles of attack/sideslip; i. e., large maneuvers of yawing / pitching channels. For skid-to-turn missile, the performance of the rolling channel pays a central role for coping with aerodynamic dynamic coupling from yawing / pitching channels. It needs not other gain adjusting logic for pitching / yawing channels.

In general, three single-input single-output (SISO) systems are designed first individually for conventional autopilot designs to get nominal gains (K_{opo}, K_{ipo}) , (K_{oq}, W_{iq}, K_{iq}) , (K_{or}, W_{ir}, K_{ir}) . And then connect them with aero-dynamic / kinematical coupling terms (see Fig.2); i.e., MIMO system, for verification the suitability of SISO designs. Several iterations are usually needed to get gain adaptive factor $Sckip$ and $Sckop$ for different values of angles of attack/sideslip. Transfer functions for analyses and designs are

$$\frac{p}{\delta p} = \frac{L_{\delta p}}{s - L_p} \quad (22)$$

for rolling channel;

$$\frac{q}{\delta q} = \frac{M_{\delta q} s - M_{\delta q} M_B Z_\alpha + Z_{\delta q} M_B Z_\alpha}{s^2 + (-M_q - M_B Z_\alpha) s + (-M_\alpha + M_q M_B Z_\alpha)} \quad (23)$$

$$\frac{a_{zcg}}{\delta q} = \frac{Z_{\delta q} s^2 - Z_{\delta q} M_q s + (M_{\delta q} Z_\alpha - Z_{\delta q} M_\alpha)}{s^2 + (-M_q - M_B Z_\alpha) s + (-M_\alpha + M_q M_B Z_\alpha)} \quad (24)$$

for pitching channel;

$$\frac{r}{\delta r} = \frac{N_{\delta r} s - N_{\delta r} M_B Y_\beta + N_{\delta r} M_B N_\beta}{s^2 + (-N_r - M_B Y_\beta) s + (N_\beta + N_r M_B Y_\beta)} \quad (25)$$

$$\frac{a_{ycg}}{\delta r} = \frac{Y_{\delta r} s^2 - Y_{\delta r} N_r s + (-N_{\delta r} Y_\beta + Y_{\delta r} N_\beta)}{s^2 + (-N_r - M_B Y_\beta) s + (N_\beta + N_r M_B Y_\beta)} \quad (26)$$

for yawing channel. The robustness specifications of the rolling channel with aerodynamic couplings from pitching/yawing channels are defined as:

1. Low frequency gain margin (LFGM) ≤ 0.707 ;
2. High frequency gain margin (HFGM) ≥ 1.707 ;
3. Phase margin(PM) $\geq 55\text{deg}$
4. Gain crossover frequency $9\text{Hz} \leq \omega_{CR} \leq 12\text{Hz}$

The break point for specification checking is at rolling inner loop. Table 1 gives final results with aerodynamic coefficient given in Appendix A, and hardware and compensators dynamics on S-domain given in Appendix B. Digital compensators are derived from bilinear transformation: $s = 2(z-1)/T_s(z+1)$ in 5-DOF simulations given in Section V. The gains $(K_{opo}, K_{ipo}, K_{oq}, W_{iq}, K_{iq}, K_{or}, W_{ir}, K_{ir})$ give in Appendix A. The bandwidths of rolling/pitching/yawing channels are $6\text{Hz}/\geq 1.1\text{Hz}/\geq 1.1\text{Hz}$; respectively. Fig.4 is frequency responses of flight conditions (A1, A4, A10) with all $(Sckip, Sckop)=(1, 1)$. A10 is the zero- coupling case, A1 is a large unstable-coupling case(LUC), and A4 is a large stable-coupling case(LSC). Fig.6 is frequency responses of flight condition (A1, A4, A10) with $(Sckip, Sckop)$ given in Table 1. From Figs.4 and 6, one can see the un-stable system becomes stable, and large gain crossover frequency is reduced after $(Sckip, Sckop)$ are introduced.

From Table 1 and Fig.5, one can see that $Sckip$ and $Sckop$ are nonlinear functions of $|A_{ZO}|$ and $|A_{YO}|$. Roughly speaking, the value of $Sckop$ is increasing for $\max(|A_{ZO}|, |A_{YO}|)$ is increasing. $Sckip$ is increasing for $|T_C|$ is increasing in unstable aerodynamic coupling while decreasing for $|T_C|$ is increasing in stable aerodynamic coupling. Note that the single-axis maneuver gives unstable aerodynamic coupling while double-axis maneuver gives stable aerodynamic coupling. Explicit formulation for $Sckip$

and $Skop$ with $|A_{ZO}|$ and $|A_{YO}|$ are very difficult and complicated. Therefore, look-up table technique with 2-D interpolation method is usually applied. In this work, Fuzzy technique with central of gravity method[21] will be applied to find $Skip$ and $Skop$. It will give a simple manner to describe zero-small-large values of maneuver $|A_{ZO}|$ or $|A_{YO}|$ and gain adaptation.

IV. The Fuzzy Gain Logic

Table 1 gives values of $Skip$ and $Skop$ for different combination of $|A_{ZO}|$ and $|A_{YO}|$ found by conventional design techniques. The maximal maneuverability of the considered system is 23G. The experience stated in Section III and zero-small-large couplings partitions given in Fig.4 can be used to formulate of fuzzy gain logic. In following formulation, $|A_{ZO}|$ and $|A_{YO}|$ are replaced by $|A_{zf}|$ and $|A_{yf}|$, respectively for on-line fuzzy logic will use measurable feedback datum $|A_{zf}|$ and $|A_{yf}|$. There are two fuzzy logics for finding $Skip$ and $Skop$, individually.

Now, consider the outer loop gain scaling factor $Skop$. Table 1 and Fig.4 give $Skop$ is function of $\max\{|A_{zf}|, |A_{yf}|\}$ and T_c . The membership function of $\max\{|A_{zf}|, |A_{yf}|\}$ is shown in Fig.7(a). It is divided into five situations: "SS", "SM", "MM", "ML", "LL"; i.e., from small through medium to large value of $\max\{|A_{zf}|, |A_{yf}|\}$. The output membership function of $Skop$ is shown in Fig.7(b). It is divided into "ZC", "SC", "LC"; i.e., from zero through small to large coupling situations. Fig.7(c) shows the fuzzy rule base.

Table 1 and Fig.4 give $Skip$ is function of $|A_{zf}|, |A_{yf}|$ and T_c . Fig.8(a) shows membership functions of $|A_{zf}|$ and $|A_{yf}|$. Fig.8(b) shows output membership function of $Skip$. Fig.8(c) shows the fuzzy rule base. Central of gravity method[21] is used to find $Skop$ and $Skip$. Off-line analyses of ten flight conditions comparing to Table 1 is given in Table 2. From Tables 1 and 2, one can see that fuzzy gain adaptation give compatible results.

V. Simulation Verifications

Figs.9 shows the 5-DOF simulating results for pitching/yawing channels commands $(A_{zc}, A_{yc}) = (-23.0G, -1.47G)$ with fuzzy gain logic. The velocity is kept at 2.0 Mach and initial altitude at 0.5Km. It is a large single-axis maneuver. The fuzzy gain logic updated rate is 50Hz. Output limitations for $(\delta pc, \delta qc, \delta rc)$ are $(\pm 5^\circ, \pm 20^\circ, \pm 20^\circ)$. This operating condition is corresponding to trim condition $(\alpha^*, \beta^*) = (12^\circ, 1^\circ)$. It gives the performance and stability of the system are satisfactory. The maximal value of rolling angular rate is equal to -15.6 deg/s . $\pm 5G$ varying testing for pitching channel command A_{zc} is applied after 4 seconds. It is corresponding to angle of attack (α^*) varying from 10° to 14° . These testing shows the fuzzy gain logic adapting $Skop$ and $Skip$ automatically, and give good performance and robustness.

Fig.10 shows simulation results for $(\alpha^*, \beta^*) = (12^\circ, 12^\circ)$. It is a large double-axis maneuver. The corresponding maneuverability are $(A_{zc}, A_{yc}) = (-23.0G, -23.0G)$. $\pm 5G$ varying testing for pitching channel command A_{zc} are applied after 4 seconds also. It gives same conclusion as the large single-axis maneuver shown in Fig.9.

VI. Conclusions

In this literature, a fuzzy flight control technique has been proposed for analyses and designs of a serious aerodynamic coupled skid-to-turn supersonic missile. Fuzzy decoupling logic was developed from conventional design techniques and experiences with two measurable accelerations. The fuzzy flight control system provides simple manner to get same robustness comparing to those of conventional designs technique. All analyzed results are verified by 5-DOF simulations under system variations and uncertainties.

References

1. Stallard, D. V., Decoupling the flight control system of a cruciform missile, AIAA- Paper- 76-1943, 1976, pp.236-246.
2. Arrow, A. and Yost, D. J., Large angle of attack missile control concepts for aerodynamic controlled missiles, J. of Spacecraft, Vol.14, No.10, 1977, pp.606-613.
3. Nesline, F. W. and Zarchan, P., Robust instrumentation configurations for homing missile flight control," AIAA Guidance Control Conference, AIAA- Paper- 80-1749, 1980, pp. 209-219.
4. Nesline, F. W. and Nesline, M. L., How autopilot requirements constraint the aerodynamic design of homing missile, American Control Conference, 1984, pp. 716-730.

5. Santis, E. and Vicino, A., diagonal dominance for robust stability of MIMO interval systems, *IEEE Transactions on Automatic Control*, Vol.41, no.6, 1996, pp.871-875.
6. Chughtai, S. S. and Munro, N., Diagonal dominance using LMIs, *IEE Proceedings- Control Theory and Applications*, Vol.151, no. 2, 2004, pp.225- 233.
7. Anderson, B. D. O. and Gevers, M. R., On multivariable pole-zero cancellations and stability of feedback systems, *IEEE Trans. on Circuit and System*, Vol. 28, No.8, 1981, pp.830-833.
8. Linnemann, A. and Maier, R., Decoupling by pre-compensation while maintaining stability, *IEEE Trans. on Automatic Control*, Vol.38, No.4, 1993, pp.629-632.
9. Wang, Q. G. and Yang, Y., Transfer function matrix approach to decoupling problem with stability, *systems and control letters*, Vol.47, 2002, pp.103-110.
10. Singh, S. N. and Rugh W. J., Decoupling in a class of nonlinear systems by state variable feedback, *Journal of Dynamic System, Measurement and Control*, Vol.94, No.4, 1972, pp.323-329.
11. Desoer, C.A. and Gunds, A. N., Decoupling linear multiinput multioutput plant by dynamic output feedback: an algebraic theory, *IEEE Trans. on Automatic Control*, Vol.31, 1986, pp.744-750.
12. Englewood, C., Snell, S. A., Enns, D. F. and Garrard, W. L., Nonlinear inversion flight control for a supermaneuver aircraft, *Journal of Guidance, Control and Dynamics* Vol.15, No.4, 1992, pp.976-984.
13. Lane, S. H. and Stengel, R. F., Flight control design using nonlinear inverse dynamics, *Automatica*, Vol. 24, 1988, pp.471-484.
14. Enns, D. D. Bugajski, R. and Stein, G., Dynamic inversion: an evolving methodology for flight control design, *Int. J. of Control*, Vol.59, 1994, pp.71-91.
15. Snell, S. A. and Stout, P. W., Flight control law using nonlinear dynamic inversion combined with quantitative feedback theory, *Journal of Dynamic Systems, Measurement and Control*, Vol.120, No.2, 1998, pp.208-214.
16. Siwakosit, W., Snell, S. A. and Hess, R. A., Robust flight control design with handling qualities Constraints using Scheduled Linear Dynamic Inversion and Loop-Shaping, *IEEE Trans. on Control Systems Technology*, Vol.8, No.3, 2000, pp.483-494.
17. Reiner, J., Balas, G. J. and Garrard, W. J., Flight control design using robust dynamic inversion and time-scale separation, *Automatica*, Vol.32, No.11, 1996, pp.1493-1504.
18. Adams R. J. and Banda, S. S., Robust flight control design using dynamic inversion and structured singular value synthesis, *IEEE Trans. on Control System Technology*, Vol.2, No.2, 1993, pp. 80-92.
19. Blakelack, J. H., *Automatic control of aircraft and missile*, Second Edition, John Wiley and Sons, New York, 1991.
20. Monta, W. J., *Supersonic aerodynamic characteristic of a sparrow III type missile model with wing control and comparison with existing tail-control results*, NASA-TR- 1078, Langley Research Center, Hampton, Virginia, 1977.
21. Passino, K. M. and Yurkovich, S., *Fuzzy control*, Addison Wesley Longman, Menlo Park, CA, 1998.

Appendix A: Aerodynamic Coefficients and Loop Gains

Ten sets(A1~A10) of aerodynamic coefficients and trim values (A_{z0} , A_{y0} , δq_0 , δr_0) of an air-to-air missile [20] at VM=676.8m/s are given below:

	$L_{\delta p}=14366$	$L_{\delta q}=431$	$L_{\delta r}=431$	$Z_{\delta q}=-28.6$
	$L_p=-3.50$	$M_q=-2.82$	$N_r=-2,82$	$Y_{\delta r}=28.6$
	$M_{\delta q}=-584$	$M_{\delta p}=-17.5$	$N_{\delta r}=-584.$	$N_{\delta p}=-17.5$
	$l_s=0.035$	$M_\beta=0.0145$	Alt = 0.5Km	Mach=2.0
	$K_{ppo}=38.95$	$K_{oq}=0.062$	$W_{iq}=28.24$	$K_{iq}=0.046$
	$K_{ipo}=0.0031$	$K_{or}=0.062$	$W_{ir}=28.24$	$K_{ir}=0.046$
A 1 .	$\alpha^*=12.0^\circ$	$\beta^*=1.00^\circ$	$L_\alpha=629.9$	$L_\beta=8238$
	$M_\alpha=-737.2$	$N_\beta=353.3$	$Z_\alpha=-183.5$	$Y_\beta=-99.5$
	$\delta q_0=-11.3^\circ$	$\delta r_0=0.46^\circ$	$A_{z0}=-23G$	$A_{y0}=-1.47G$
A 2 .	$\alpha^*=12.0^\circ$	$\beta^*=4.00^\circ$	$L_\alpha=2665$	$L_\beta=3533$
	$M_\alpha=-737.2$	$N_\beta=353.3$	$Z_\alpha=-183.5$	$Y_\beta=-113.4$
	$\delta q_0=-11.6^\circ$	$\delta r_0=2.19^\circ$	$A_{z0}=-23G$	$A_{y0}=-5.96G$
A 3 .	$\alpha^*=12.0^\circ$	$\beta^*=8.00^\circ$	$L_\alpha=5552$	$L_\beta=-4382$
	$M_\alpha=-737.2$	$N_\beta=634.9$	$Z_\alpha=-183.5$	$Y_\beta=-167.7$
	$\delta q_0=-11.6^\circ$	$\delta r_0=6.32^\circ$	$A_{z0}=-23G$	$A_{y0}=-13.5G$
A 4 .	$\alpha^*=12.0^\circ$	$\beta^*=12.00^\circ$	$L_\alpha=6838.8$	$L_\beta=-6838.8$
	$M_\alpha=-737.2$	$N_\beta=737.2$	$Z_\alpha=-183.5$	$Y_\beta=-183.5$
	$\delta q_0=-11.6$	$\delta r_0=11.6$	$A_{z0}=-23G$	$A_{y0}=-23G$
A 5 .	$\alpha^*=8.0^\circ$	$\beta^*=1.00^\circ$	$L_\alpha=574.1$	$L_\beta=5327$
	$M_\alpha=-634.9$	$N_\beta=276.6$	$Z_\alpha=-167.7$	$Y_\beta=-183.5$
	$\delta q_0=-6.3^\circ$	$\delta r_0=0.47^\circ$	$A_{z0}=-13.5G$	$A_{y0}=-1.47G$
A 6 .	$\alpha^*=8.0^\circ$	$\beta^*=4.00^\circ$	$L_\alpha=3392$	$L_\beta=-332$
	$M_\alpha=-634.9$	$N_\beta=353.3$	$Z_\alpha=-167.7$	$Y_\beta=-113.4$
	$\delta q_0=-6.3$	$\delta r_0=2.19$	$A_{z0}=-13.5G$	$A_{y0}=-5.96G$
A 7 .	$\alpha^*=8.0^\circ$	$\beta^*=8.00^\circ$	$L_\alpha=5757$	$L_\beta=5757$
	$M_\alpha=-634.9$	$N_\beta=634.9$	$Z_\alpha=-167.7$	$Y_\beta=-167.7$
	$\delta q_0=-6.32^\circ$	$\delta r_0=6.32^\circ$	$A_{z0}=-13.5G$	$A_{y0}=-13.5G$
A 8 .	$\alpha^*=4.0^\circ$	$\beta^*=1.00^\circ$	$L_\alpha=558$	$L_\beta=2609$
	$M_\alpha=-353.3$	$N_\beta=276.6$	$Z_\alpha=-113.4$	$Y_\beta=-99.6$
	$\delta q_0=-2.19$	$\delta r_0=0.47$	$A_{z0}=-5.96G$	$A_{y0}=-1.47G$
A 9 .	$\alpha^*=4.0^\circ$	$\beta^*=4.00^\circ$	$L_\alpha=-3435$	$L_\beta=3435$
	$M_\alpha=-353.3$	$N_\beta=353.3$	$Z_\alpha=-113.4$	$Y_\beta=-113.4$
	$\delta q_0=-2.19^\circ$	$\delta r_0=2.19^\circ$	$A_{z0}=-5.96G$	$A_{y0}=-5.96G$
A 10 .	$\alpha^*=1.0^\circ$	$\beta^*=1.00^\circ$	$L_\alpha=-2567$	$L_\beta=-2567$
	$M_\alpha=-276.6$	$N_\beta=276.6$	$Z_\alpha=-99.6$	$Y_\beta=-99.6$
	$\delta q_0=0.47^\circ$	$\delta r_0=0.47^\circ$	$A_{z0}=-1.47G$	$A_{y0}=-1.47G$

Appendix B: Compensators and Hardware Dynamic Models

1. Rolling outer/inner loop compensators

$$POC(s) = \frac{s/8.79+1}{s/4.4+1}, PIC(s) = \frac{s/282.6+1}{s/1413+1}$$

2. Yawing/Pitching outer/inner loop compensators

$$ROC(s) = \frac{s/18.84+1}{s/12.56+1}, RIC(s) = \frac{s/157+1}{s/942+1}, QOC(s) = \frac{s/18.84+1}{s/12.56+1}, QIC(s) = \frac{s/157+1}{s/942+1}$$

3. Actuator models

$$CAS(s) = \frac{166627}{s^2 + 142.95s + 166627}$$

4. Rate gyro/accelerometer models

$$RG(s) = \frac{193444}{s^2 + 263.9s + 193444}$$

5. Inner loop low-pass filter body angular rate

$$LPFI(s) = \frac{439.6}{s + 439.6}$$

6. Outer loop low-pass filter for acceleration

$$LPFO(s) = \frac{251.2}{s + 251.2}$$

Table 1. Rolling channel design results with gain logic.

Trims	Maneuvers	Gain Scaling		Robustness			
		<i>Azo / Ayo(G)</i>	<i>Sckop</i>	<i>Sckip</i>	LFGM	HFGM	PM(°)
1°/1°	-1.47/-1.47	1.00	1.00	∞	2.35	65.0	10.2
4°/1°	-5.96/-1.47	1.12	1.10	0.19	2.24	63.3	10.6
8°/1°	-13.5/-1.47	1.30	1.23	0.43	2.00	60.4	10.6
12°/1°	-23.0/-1.47	1.50	1.45	0.68	1.72	56.9	10.6
4°/4°	-5.96/-5.96	1.12	0.90	∞	2.72	63.9	10.3
4°/8°	-5.96/-13.5	1.30	1.00	∞	2.45	61.7	10.9
4°/12°	-5.96/-23.0	1.50	1.20	0.37	2.05	58.3	11.0
8°/8°	-13.5/-13.5	1.30	0.70	∞	3.44	65.6	11.1
8°/12°	-13.5/-23.0	1.50	0.72	∞	3.33	63.2	11.5
12°/12°	-23.0/-23.0	1.50	0.50	∞	4.74	69.2	11.9

Table 2. Rolling channel design results with fuzzy gain logic.

Trims	Maneuvers	Gain Scaling		Robustness			
		<i>Azo / Ayo(G)</i>	<i>Sckop</i>	<i>Sckip</i>	LFGM	HFGM	PM(°)
1°/1°	-1.47/-1.47	1.04	1.04	∞	2.35	65.0	10.7
4°/1°	-5.96/-1.47	1.14	1.14	0.19	2.16	63.4	11.0
8°/1°	-13.5/-1.47	1.29	1.21	0.44	2.04	60.3	10.4
12°/1°	-23.0/-1.47	1.51	1.43	0.69	1.74	56.3	10.3
4°/4°	-5.96/-5.96	1.14	0.85	∞	2.89	63.2	9.8
4°/8°	-5.96/-13.5	1.29	1.01	∞	2.43	62.0	10.9
4°/12°	-5.96/-23.0	1.51	1.22	0.36	2.02	58.4	11.2
8°/8°	-13.5/-13.5	1.29	0.77	∞	3.13	65.3	11.6
8°/12°	-13.5/-23.0	1.51	0.71	∞	3.36	63.2	11.4
12°/12°	-23.0/-23.0	1.51	0.50	∞	4.72	69.1	11.9

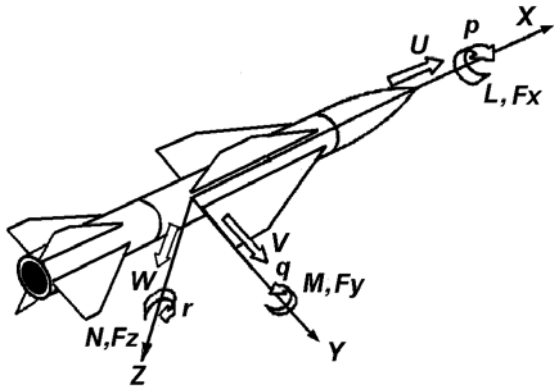


Fig.1 Coordinated system definitions.

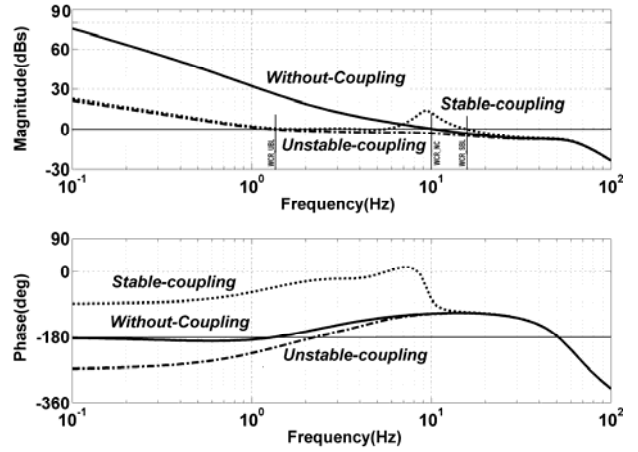


Fig.4 Open-loop frequencies of unstable/stable/zero aerodynamic couplings.

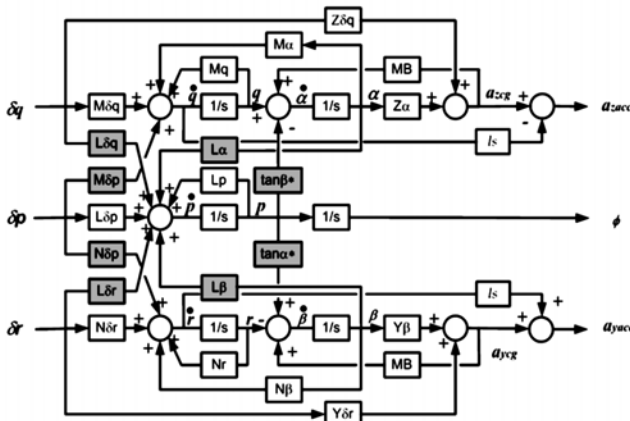


Fig.2 Linear perturbed model of the missile with trims (α^* , β^*).

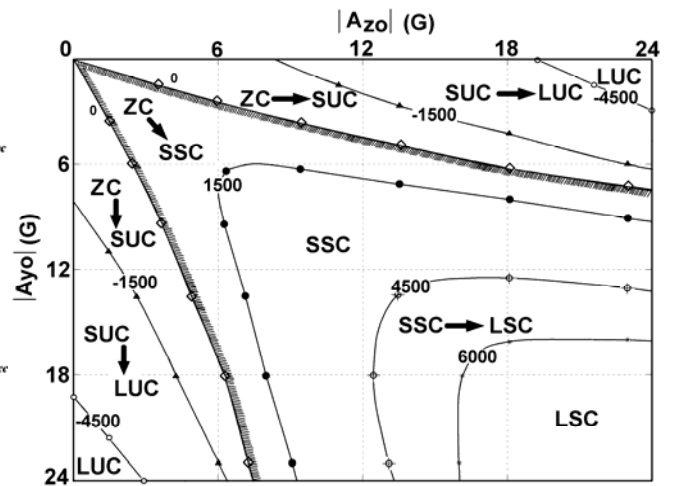


Fig.5 Classification for stable/unstable couplings.

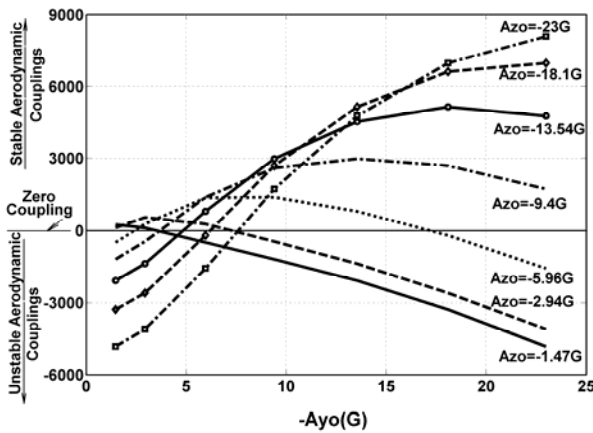


Fig.3 Couplings (T_C) from pitching/yawing channels to rolling channel.

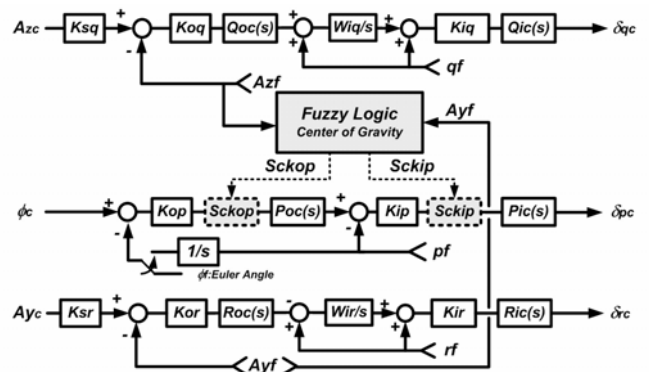


Fig.6 Autopilot configuration with fuzzy gain logic.

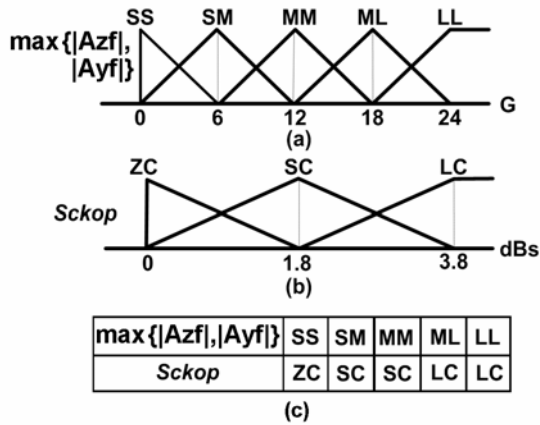


Fig.7 (a) Membership function of maneuverability.
 (b) Membership function of *Sckop*.
 (c) Fuzzy rule base.

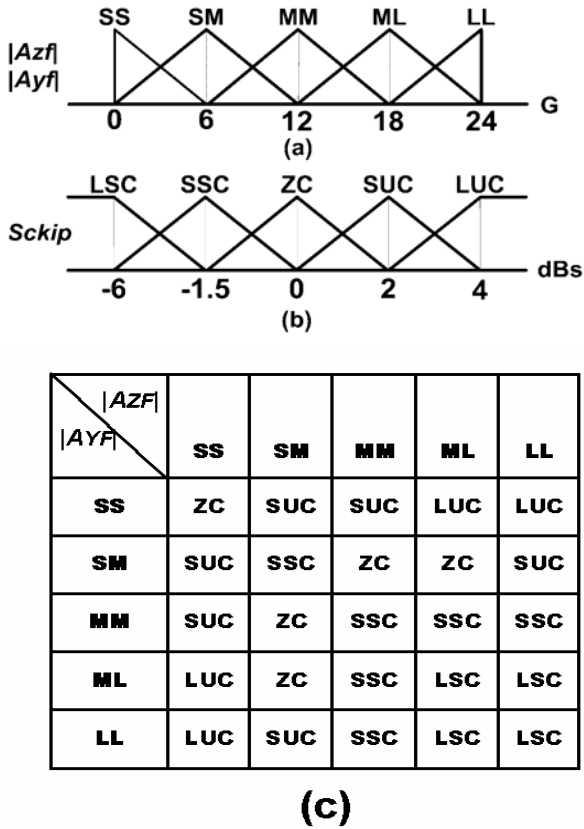


Fig.8 (a) Membership of maneuverabilities.
 (b) Membership of *Sckip*.
 (c) Fuzzy rule base.

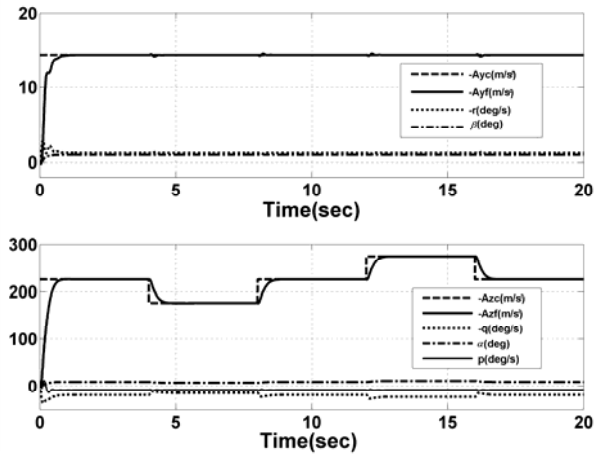


Fig.9 5-DOF simulation of a large single-axis $(Azc,Ayc)=(-23G,-1.47G)$ Maneuvering.

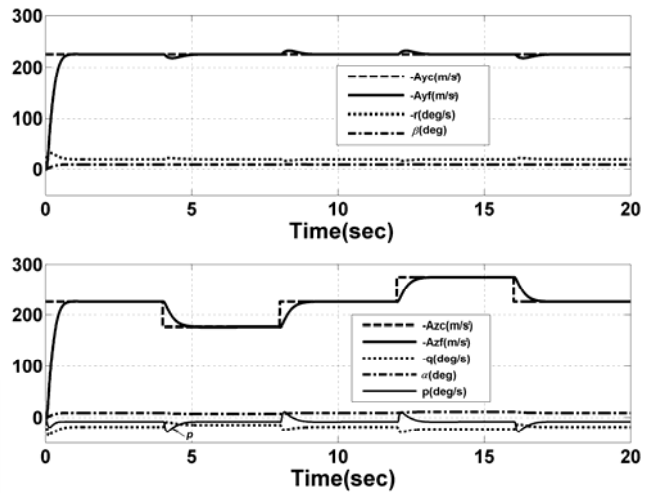


Fig.10 5-DOF simulation of a large double-axis $(Azc,Ayc)=(-23G,-23G)$ maneuvering.

超音速飛彈之解藕連模糊控制系統設計

蔡添壽

國立虎尾科技大學飛機工程學系 助理教授

摘 要

本文根據傳統飛行控制系統設計技術與經驗，提出模糊解藕連飛行控制系統設計，模糊控制法則的兩個輸入參數為可量測的加速度資料，此模糊控制法則可以簡單的被運用來對付單軸與雙軸大操縱命令飛行操作，得到的結果與傳統的設計相當，但方法較簡單，不需要多維增益值查表，所有的分析結果都經含不確定性與大系統變異之五自由度飛行模擬驗證。

關鍵詞: 模糊控制、飛行控制系統、氣動力解藕。

國立虎尾科技大學飛機工程學系，雲林縣63208虎尾鎮文化路64號。

Tel:+886-5-631-5537

Fax:+886-5-631-2415

E-mail: ttsy@nfu.edu.tw

